

# Bandlimited Signal Extrapolation Using Prolate Spheroidal Wave Functions

Amal Devasia<sup>1</sup> and Michael Cada<sup>2</sup>

**Abstract**— A simple, efficient and reliable method to extrapolate bandlimited signals varying from lower to higher frequencies is proposed. The orthogonal properties of linear prolate spheroidal wave functions (PSWFs) are exploited to form an orthogonal basis set needed for synthesis. A significant step in the process is the higher order piecewise polynomial approximation of the overlap integral required for obtaining the expansion coefficients accurately with very high precision. Two sets of PSWFs, one relatively with lower Slepian frequency and the other with higher Slepian frequency, are considered. Numerical results of extrapolation of some standard test signals using the two sets are presented, compared, discussed, and some interesting inferences are made.

**Index Terms**—Signal extrapolation; Slepian series; Bandlimited signals; Linear prolate spheroidal wave functions; Overlap integral; High-precision numerical integration

## I. INTRODUCTION

A remarkable discovery was made about half a century ago by David Slepian, an American mathematician, and his colleagues on a special set of functions called prolate spheroidal wave functions (PSWFs). These functions, also known as Slepian prolate functions, were bandlimited and exhibited interesting orthogonality relations. They are normalized versions of the solutions to Helmholtz wave equation [1] in spheroidal coordinates. In his paper [2-5], Slepian proposed the idea of bandlimited signal extrapolation using PSWFs. Generating this set of functions practically seemed difficult because of the complexity involved and limited computational capabilities existed. Hence, there hasn't been any significant interest in this field up until very recently. However, with advanced numerical techniques and superior computational power, there has been noticeable activity in this field within the past decade [6-9]. In [10], Senay *et al.* proposed sampling and reconstruction of bandlimited as well as non-bandlimited signals using Slepian functions. They discussed the idea of modifying the Whittaker-Shannon sampling theory by replacing the *sinc* basis by Slepian functions for

reconstruction of signals. Further to this, in [11,12], they showed signal reconstruction using non-uniform sampling and level-crossing sampling with Slepian functions.

Since the primary focus of this paper is on bandlimited signal extrapolation and not just reconstruction or interpolation, we will concentrate more on the recent advancements in this regard. While we consider the signals to be bandlimited in the Fourier transform domain, much attention has recently been on extrapolation of signals bandlimited in linear canonical transform (LCT) domain, this being a four-parameter family of linear integral transform [13,14] that generalizes Fourier transform as one of its special cases. For extrapolation of LCT bandlimited signals, several iterative and non-iterative algorithms have been proposed [15-18]. Most of the iterative algorithms are centered on modifying the Gerchberg-Papoulis (GP) algorithm [19,20] that relies on successive reduction of error energy. Although theoretical convergence of the result has been shown, there is still some uncertainty associated with the swiftness with which this is achieved. With respect to the non-iterative algorithms proposed in [16], the authors themselves admit that the extrapolation could become unstable with an increase in the number of observations. A comparison of the extrapolation of an LCT bandlimited signal, using an iterative GP algorithm and another algorithm based on signal expansion into a series of generalized PSWFs [18] is presented in [17]. The comparison showed better results for the iterative method proposed in [17] over the one described in [18], in terms of the normalized mean square error (NMSE). Gosse, in [21], performed Fourier bandlimited signal extrapolation by handling lower and higher frequencies of the signal separately. He used PSWFs for extrapolating lower frequency components while the higher frequencies were dealt with compressive sampling [22,23] algorithms. The efficiency of the proposed method was highly dependent on the correlation between low and high frequencies in the signal (it should be weak for better results), the existence of a sparse representation of higher frequencies in the Fourier basis, and on a reasonable choice of extrapolation domain.

In this paper, we propose a non-iterative and simple method for extrapolating bandlimited signals varying from relatively lower to higher frequencies using Slepian functions. Although we concentrate mainly on Fourier bandlimited signals, it however might also be applied for LCT bandlimited cases as is shown in one of our results below. Several comparisons are made with the results obtained in earlier related publications. They show that, within the prescribed bandwidth, the proposed method is far superior over several other methods referenced in this paper. PSWFs for analysis purposes need to be computed

Manuscript received November 25, 2013. This work was supported in part by Applied Science in Photonics and Innovative Research in Engineering (ASPIRE), a program under Collaborative Research and Training Experience (CREATE) program, funded by Natural Sciences and Engineering Research Council (NSERC) of Canada.

<sup>1</sup> Amal Devasia is a MAsc. candidate in the Department of Electrical and Computer Engineering, Dalhousie University, Halifax, NS, B3H 4R2, Canada (e-mail: [amal.devasia@dal.ca](mailto:amal.devasia@dal.ca)).

<sup>2</sup> Michael Cada is with the Department of Electrical and Computer Engineering, Dalhousie University, Halifax, NS, B3H 4R2, Canada (e-mail: [michael.cada@dal.ca](mailto:michael.cada@dal.ca)).

accurately and with rather high precision. Here, we rely on a proprietary algorithm developed theoretically and implemented numerically by Cada [24], for accurately generating the linear prolate functions (one-dimensional PSWFs, henceforth abbreviated as LPFs) set with desired high precision. Once the LPFs set is obtained with the corresponding eigenvalues (discussed later in this paper), they are employed in our algorithm for extrapolation. Here, we do not consider the storage of LPFs set as an issue (as put forward by Shi *et al.* in [17]) to be addressed, as it is not the subject of this paper.

Cada's algorithm exploits robust properties of certain formulae derived that are efficient, accurate and suitable for fast numerical evaluations of linear prolate functions and their eigenvalues. Previous methods [Slepian, Flammer [25], etc.] required lengthy cumbersome calculations with slowly converging series and necessary approximations that led to insurmountable numerical problems and/or failing when higher orders were concerned. Prolate functions and the eigenvalues change their properties drastically at certain parameter values (see below), which has caused described problems. Even standard professional high-quality commercial packages such as Mathematica or Matlab fail to compute these functions and eigenvalues correctly or at all for such a combination of parameters that is critical for extrapolation applications. Our algorithm enables to break through this numerical barrier and makes it possible to calculate linear prolate functions and their eigenvalues correctly for basically any parameters.

Signal extrapolation is an extension of a signal,  $f(t)$ , beyond the interval in which it is known to the observer. Symbolically, we can represent it as:

$$f(t) = \begin{cases} \text{known}, & |t| \leq t_0 \\ \text{unknown (extrapolation)}, & |t| > t_0 \end{cases} \quad (1)$$

The region in which the signal is known is called the observation interval (here,  $[-t_0, t_0]$ ). Bandlimited signals are bound in the frequency domain; their Fourier transform,  $F(\omega)$ , vanishes beyond a particular finite frequency interval. Thus if,

$$F(\omega) = 0, \quad |\omega| > \Omega, \quad (2)$$

then  $f(t)$  is said to be  $\Omega$ -bandlimited.

The following sections of the paper are organized as follows. In section II, LPFs and their relevant properties are discussed. The various steps involved in our proposed extrapolation algorithm are described throughout in section III. Section IV is devoted to presenting the actual extrapolated results of various test functions, their comparison and error analysis. Finally, in section V, we conclude with our inferences and possible future prospects.

## II. PRELIMINARIES

The theoretical treatment of bandlimited signal extrapolation using PSWFs was first discussed by Slepian and his colleagues in [2]. They explained the use of PSWFs, or more precisely, linear prolate functions (LPFs) as an orthogonal basis set for decomposition and reconstruction of the signal using analysis and synthesis equations. Linear

prolate functions are one-dimensional PSWFs denoted by  $\Psi_n(c, t)$ , where  $n$  is the order of LPF (non-negative integer),  $t$  is the time parameter and  $c$  is the bandwidth parameter also known as Slepian frequency. LPFs can be evaluated using:

$$\Psi_n(c, t) = \frac{\sqrt{\lambda_n(c)/t_0}}{\sqrt{\int_{-1}^1 (S_{0n}(c, t))^2 dt}} S_{0n}\left(c, \frac{t}{t_0}\right), \quad (3)$$

where  $\lambda_n(c)$  is the eigenvalue of *sinc* kernel with  $\Psi_n(c, t)$  as eigenfunction (a measure of concentration of signal in the observation interval  $[-t_0, t_0]$ ),  $t_0$  is the observation boundary of the interval in which the function is known, and  $S_{m,n}(c, \eta)$  are the angular solutions of the first kind to Helmholtz wave equation. The eigenvalue  $\lambda_n(c)$  is given by,

$$\lambda_n(c) = \frac{2c}{\pi} [R_{0,n}(c, 1)]^2, \quad (4)$$

where  $R_{m,n}(c, \varepsilon)$  are the radial solutions of the first kind to Helmholtz wave equation.

Numerical evaluation of the LPFs set along with their corresponding eigenvalues practically seemed very difficult as it involved finding precise numerical values of the angular ( $S_{m,n}(c, \eta)$ ) and radial ( $R_{m,n}(c, \varepsilon)$ ) solutions. For obtaining this, a typical power series expansion was used which was predetermined by the association of Legendre and spherical Bessel functions to the angular and radial solutions respectively. Interested readers are referred to [8,9,26] for more details on LPFs derivation. These LPFs along with their corresponding eigenvalues have been used in our extrapolation algorithm. It should be noted that since extrapolation relies heavily on values of  $\Psi_n$ 's and  $\lambda_n$ 's when  $n > 2c/\pi$ , it is of paramount importance that one computes them accurately and with high precision. Ours is the first algorithm that offers such a capability.

### A. Properties of LPFs

LPFs have many interesting properties of which some of the relevant ones related to this study are shown below.

#### (i) Bandlimited

Bandlimiting property of LPFs is denoted by a free bandwidth parameter (Slepian frequency)  $c$  given by:

$$c = \Omega_0 t_0, \quad (5)$$

where  $\Omega_0$  is the finite bandwidth of  $\Psi_n(c, t)$  for a given order  $n$ .

#### (ii) Symmetry

LPFs exhibit even and odd symmetries based on their integer order  $n$ . If  $n$  is even,  $\Psi_n(c, t)$  is even symmetric. If  $n$  is odd, then it is odd symmetric (see Figure 1).

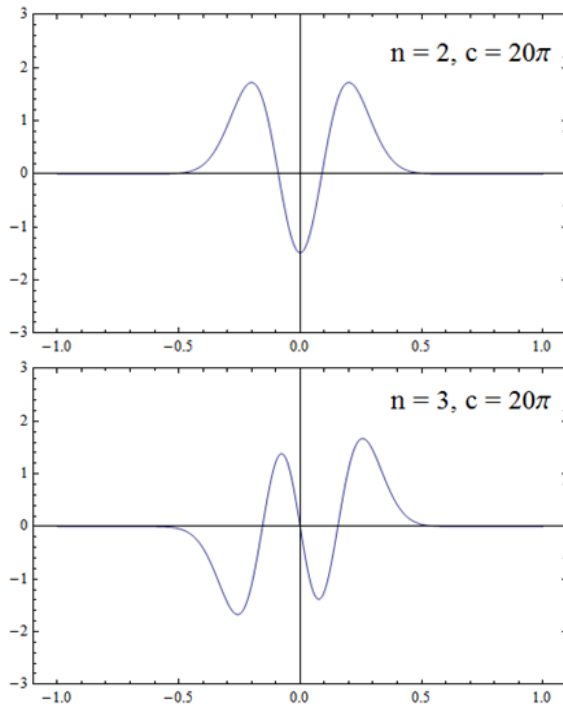


Figure 1. Even (top) and odd (bottom) symmetries of  $\Psi_n(c, t)$  for  $c = 20\pi$ .

### (iii) Orthogonality

LPFs are linearly independent and orthogonal over finite (6) as well as infinite (7) intervals, unlike, for example, trigonometric functions that are orthogonal only over a finite domain.

$$\int_{-t_0}^{t_0} \Psi_n(c, t) \Psi_m(c, t) dt = \begin{cases} \lambda_n(c) & \text{for } n = m, \\ 0 & \text{otherwise.} \end{cases} \quad (6)$$

$$\int_{-\infty}^{\infty} \Psi_n(c, t) \Psi_m(c, t) dt = \begin{cases} 1 & \text{for } n = m, \\ 0 & \text{otherwise.} \end{cases} \quad (7)$$

where  $n, m$  are non-negative integers.

### (iv) Invariance to Fourier transforms

Fourier transforms of LPFs over both finite (8) and infinite (9) intervals are simply scaled versions of themselves.

$$\int_{-t_0}^{t_0} \Psi_n(c, t) e^{j\omega t} dt = j^n \left( \frac{2\pi\lambda_n(c)t_0}{\Omega_0} \right)^{1/2} \Psi_n \left( c, \frac{\omega t_0}{\Omega_0} \right) \quad (8)$$

$$\int_{-\infty}^{\infty} \Psi_n(c, t) e^{j\omega t} dt = j^n \left( \frac{2\pi t_0}{\Omega_0} \right)^{1/2} \Psi_n \left( c, \frac{\omega t_0}{\Omega_0} \right) \quad (9)$$

Expressions (8) and (9) show LPFs' invariance to Fourier transforms and are a further proof of their bandlimiting property.

## III. EXTRAPOLATION ALGORITHM

Starting from the theory and going through various numerical techniques involved, this section explains the steps with which we implemented our extrapolation algorithm.

### A. Analysis and synthesis

Generally speaking, any bandlimited signal can be

decomposed into a linear combination of weighted orthogonal basis functions using the relation:

$$f(t) = \sum_{n=-\infty}^{\infty} \gamma_n \Phi_n(t) \quad (\text{synthesis}), \quad (10)$$

where  $f(t)$  is the signal,  $\gamma_n$  is a set of scalar coefficients, and  $\Phi_n(t)$  is the orthogonal basis set.

The set of scalar coefficients is found from:

$$\gamma_n = \frac{\int_{-\infty}^{\infty} f(t) \Phi_n(t) dt}{\int_{-\infty}^{\infty} \Phi_n(t) \Phi_n(t) dt} \quad (\text{analysis}). \quad (11)$$

Employing LPFs as the orthogonal basis set for a fixed Slepian frequency  $c$  yields:

$$\gamma_n(c) = \lambda_n^{-1}(c) \int_{-t_0}^{t_0} f(t) \Psi_n(c, t) dt \quad (\text{analysis}), \quad (12)$$

where  $\int_{-t_0}^{t_0} f(t) \Psi_n(c, t) dt$  is known as the overlap integral, and  $\gamma_n(c)$  are the scalar expansion coefficient for a given order  $n$  of LPF.

The synthesis equation, used for signal extrapolation, is given by:

$$f(t) \cong \sum_{n=0}^N \gamma_n(c) \Psi_n(c, t) \quad (\text{synthesis}), \quad (13)$$

where  $N$  is the truncation value for the order  $n$ .

The above equations (12) and (13) form the backbone of our signal extrapolation algorithm.

### B. LPFs set

Two distinct sets of LPFs were used as potential orthogonal basis sets for the proposed algorithm. These functions were discretized in time for numerical implementation. Each of these sampled data has very high numerical precision of about 200 digits. The two sets vary in their Slepian frequency; the specifics are as follows:

#### ( $\Psi_n(c, t)$ Set 1)

$c = 20\pi, n: 0 \rightarrow 101, t \rightarrow [-1.900, 1.900]$  (see Figure 2).

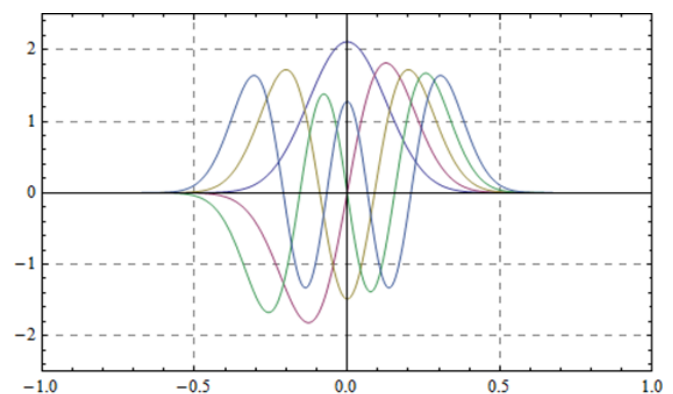


Figure 2. LPFs set 1 ( $c = 20\pi, n: 0 \rightarrow 4$ ).

#### ( $\Psi_n(c, t)$ Set 2)

$c = 100\pi, n: 0 \rightarrow 601, t \rightarrow [-1.900, 1.900]$  (see Figure 3).

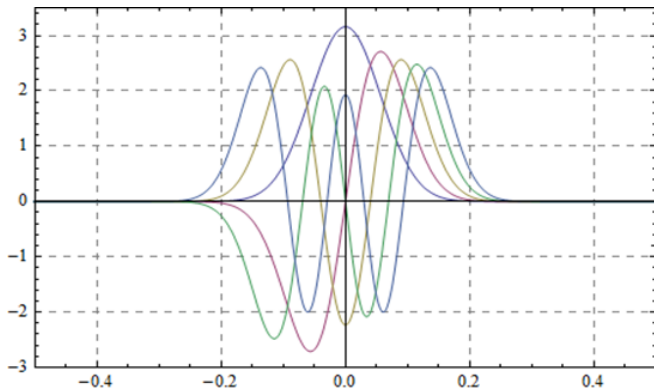


Figure 3. LPFs set 2 ( $c = 100\pi, n: 0 \rightarrow 4$ ).

The time parameter  $t$  is specified with 3 digits of precision after the decimal point as the sampling period in the time axis is  $0.001s$ . Generally, for any LPFs set with a fixed  $c$ , as the order  $n$  increases, the concentration of the LPFs within  $[-t_0, t_0]$  decreases. For  $n = 2c/\pi$ , the signal's maximum concentration reaches the boundary of the observation interval (see Figure 4).

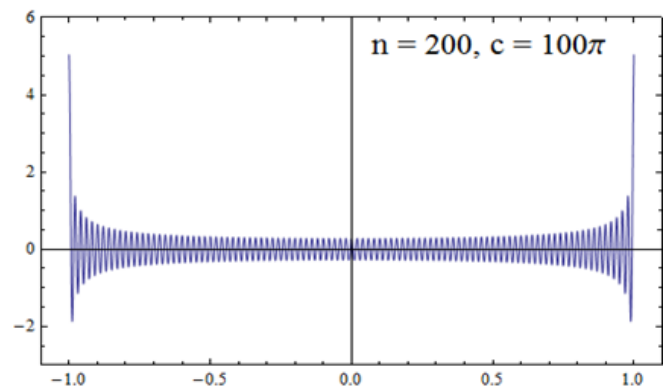
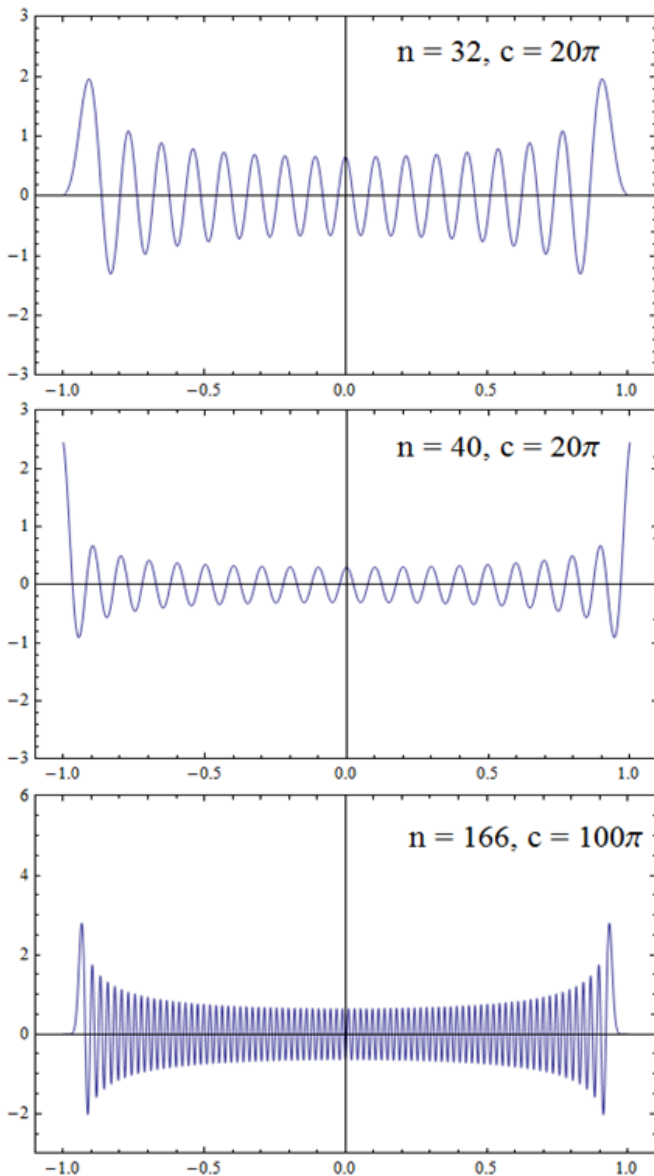


Figure 4. Dependency of signal concentration on the order  $n$  for LPFs set 1 (top two) and 2 (bottom two).

### C. Overlap integral

By taking a closer look at the analysis (12) and synthesis (13) equations using LPFs, one can notice that  $f(t)$ , the function to be extrapolated, is well defined in  $[-t_0, t_0]$ , i.e.  $[-1,1]$  ( $t_0$  chosen to be 1). Numerical values of  $\lambda_n(c)$  and  $\Psi_n(c, t)$  as a set for a given  $c$  are also known (see section II). The only unknown factor is an efficient method to calculate the overlap integral given by  $\int_{-1}^1 f(t) \Psi_n(c, t) dt$ . Efficient estimation of overlap integral is of paramount importance in obtaining accurate results for extrapolation. As LPFs,  $\Psi_n(c, t)$ , and eigenvalues,  $\lambda_n(c)$ , are required to be of high precision for high orders of  $n$ , the eigenvalues tend to become extremely small, close to zero, which makes this essentially a problem of high precision numerical integration. If and when computed inaccurately, the coefficients of expansion,  $\gamma_n(c)$ , of the synthesis equation (13) assume extremely large values for such  $n$ 's that are crucial and irreplaceable for extrapolation purposes. This, in turn, causes enormous numerical errors that thus render extrapolated signals completely incorrect and useless.

### D. Calculation of overlap integral

A simple and efficient way to compute overlap integral is proposed and implemented to obtain satisfactory results. To make it simple and generic, polynomial approximation of the discrete samples of the scalar product  $f(t) \Psi_n(c, t)$  was chosen. Our primary focus was to obtain the right polynomial approximation for the underlying common function,  $\Psi_n(c, t)$  (for a given  $c$ ), in any scalar product, irrespective of the bandlimited function  $f(t)$ . Another major task was to choose the right truncation value  $N$  for synthesis (13), which we determined by examining the behavior of the scalar coefficients  $\gamma_n(c)$  obtained in analysis (12). After a series of thorough investigations using different kinds of polynomial interpolation and numerical integration techniques, it was found that piecewise polynomial approximation is best suited for the particular LPF sets that were used.

Direct method of piecewise polynomial interpolation [27] is used. Given  $k$  discrete data points,  $(x_0, y_0)$  to  $(x_{k-1}, y_{k-1})$ , it can be approximated to a polynomial of order  $k - 1$  as:

$$y = \beta_0 + \beta_1 x + \dots + \beta_{k-1} x^{k-1}, \quad (14)$$

where the coefficients ( $\beta$ ) can be found by solving this linear system of equations:

$$\begin{pmatrix} y_0 \\ y_1 \\ \vdots \\ y_{k-1} \end{pmatrix} = \begin{pmatrix} 1 & x_0 & x_0^2 & \cdots & x_0^{k-1} \\ 1 & x_1 & x_1^2 & \cdots & x_1^{k-1} \\ \vdots & \vdots & \vdots & \ddots & \vdots \\ 1 & x_{k-1} & x_{k-1}^2 & \cdots & x_{k-1}^{k-1} \end{pmatrix} \begin{pmatrix} \beta_0 \\ \beta_1 \\ \vdots \\ \beta_{k-1} \end{pmatrix}. \quad (15)$$

Relating this approach to the problem at hand, there are 1001 samples in the time interval  $[0,1]$  and 2001 samples in  $[-1,1]$ . The whole interval of  $[-1,1]$  is divided into 8 equal segments, thus there are 251 samples in each segment of the samples of the scalar product  $f(t) \Psi_n(c, t)$ . Applying piecewise polynomial approximation to each segment containing 251 samples, one obtains a polynomial of order 250 for each segment. Simply integrating each segment yields the desired overlap integral.

#### IV. RESULTS AND DISCUSSION

Mathematica, a software tool that is well suited for high precision computing, has been used for implementing our algorithm. Extrapolation was carried out for some selected known test functions using both LPFs set 1 and 2; some results of which extrapolated using LPFs set 1 can also be found in [28] and is used here for making comparisons and drawing conclusions. The only restriction imposed on the selected signals was that its maximum frequency should be less than or equal to that of the corresponding LPFs set used for their extrapolation. In the results shown below, the same extrapolation formula was employed for both reconstructing the signal within as well as extrapolating it beyond the interval  $[-1,1]$ . To show the error estimates with respect to the original signal, common logarithm of the absolute error between the extrapolated and original data is also plotted. Extrapolation errors of the order of up to  $10^{-2}$  or  $10^{-3}$  are considered acceptable.

Upon careful inspection of the plots in Figures 9, 10 and 11, 12, one could notice that when the same signal was extrapolated using the two LPF sets, the higher Slepian frequency set (set 2) was more accurate in their approximations (see the logarithm of absolute error plots) within their effective extrapolation range. The signals for which the extrapolation is shown in Figure 5 and 6, although not exactly bandlimited because of the Gaussian functions involved, also gave good results (as seen in Figure 6), which are comparable to what was achieved using strictly bandlimited cases (Figure 7, 8 and 11).

As expected, the effective extrapolation range was higher for the lower  $c$  LPFs set (set 1) as compared to the higher  $c$  LPFs set (set 2). The range of extrapolation is limited mainly due to the series truncation,  $N$ , the value of which should be at least greater than  $2c/\pi$  for performing extrapolation. We also verified the effective extrapolation range that can be achieved analytically by using simple sinusoidal signals, for which the analytical expressions are known [8]. We found that using LPFs set 1, the truncation value  $N$  was mostly equal to 100 (out of the total order of  $n = 101$  being considered), while using LPFs set 2 it was more or less close to 300 (out of  $n = 601$ ); both greater than

their corresponding  $2c/\pi$  values, thus allowing signal extrapolation.

However, it is worth mentioning at this point that what we considered here as the lower frequency set has been regarded as, or included in, the higher frequency group by Gosse in [21]. The effective extrapolation range in our case is significantly improved when compared with their results for the same signal (see [21], page 1277; and Figure 5 of this paper). In the same context, the error analysis also shows better results as our method has absolute error magnitude around  $10^{-38}$  (while it is  $10^{-2}$  in [21]) within the reconstruction interval  $[-1,1]$ . We also obtained better ratios of error magnitudes (varying smoothly from the order of  $10^{-36}$  to  $10^{-3}$  using our algorithm, while oscillating between  $10^{-2}$  and  $10^{-1}$  in [21]) in the effective extrapolation region, i.e. outside  $[-1,1]$  (see absolute error plots of Figure 5).

$$1) f_1(t) = e^{-2t^2} e^{3t} \sin(\pi t) \cos(3\pi t) + 0.5[\sin(5\pi t) - \cos(7\pi t)]$$

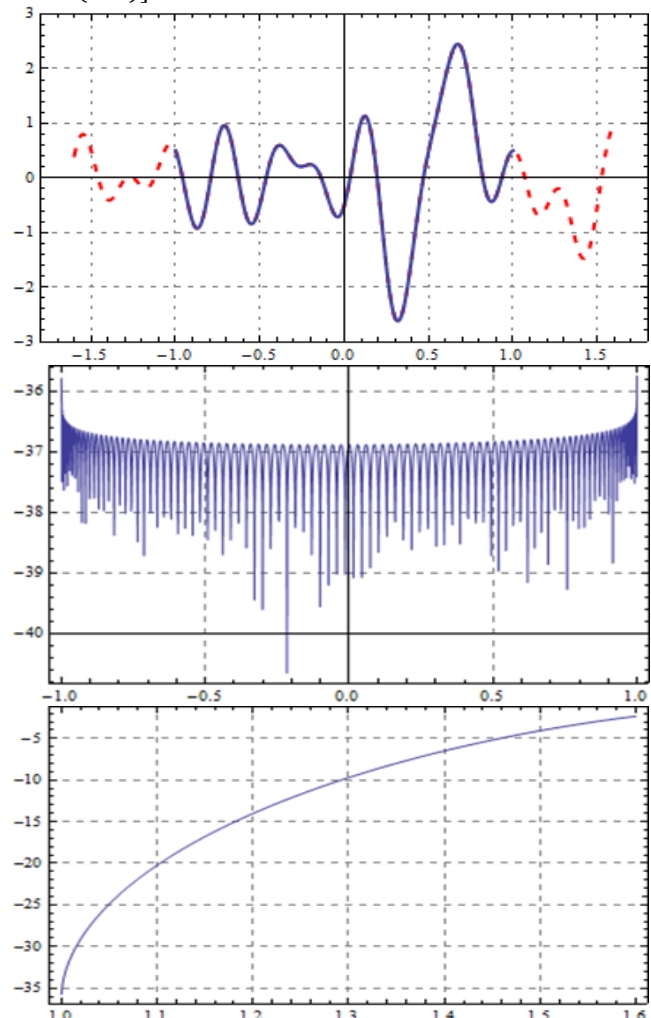


Figure 5.  $f_1(t)$  original [solid] and extrapolated [dashed] (top), logarithm of absolute error (bottom two) versus time; LPFs set 1 used.

$$2) f_2(t) = 3 \sin\left(17\pi t + \left(\frac{\pi}{5}\right)\right) - 5 \cos\left(13\pi t - \left(\frac{3\pi}{8}\right)\right) - 2e^{-\pi(t+7)^2} + 9e^{-\pi t^2}$$

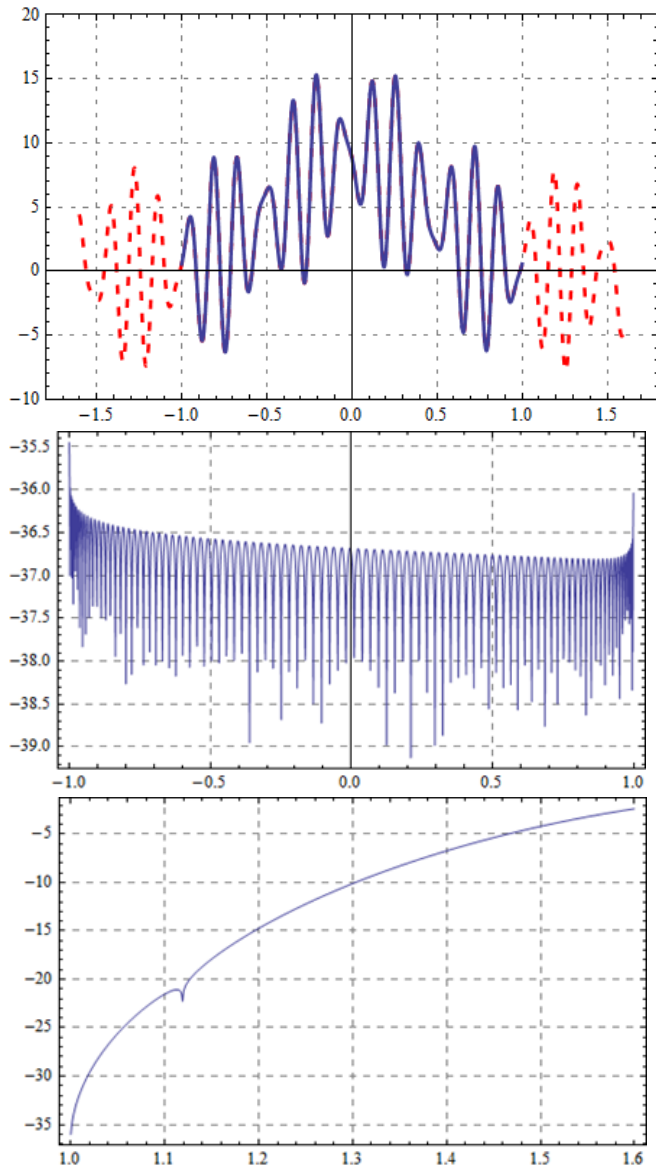


Figure 6.  $f_2(t)$  original [solid] and extrapolated [dashed] (top), logarithm of absolute error (bottom two) versus time; LPFs set 1 used.

$$3) f_3(t) = \cos\left(20\pi t - \left(\frac{\pi}{11}\right)\right) + \cos\left(\frac{20\pi t}{7}\right) - \cos\left(\frac{15\pi t}{2}\right)$$

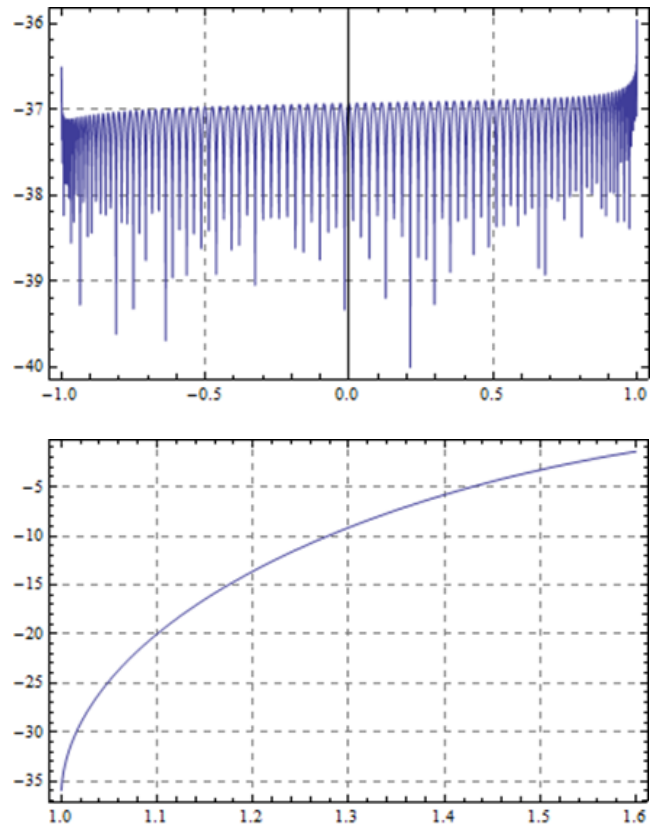
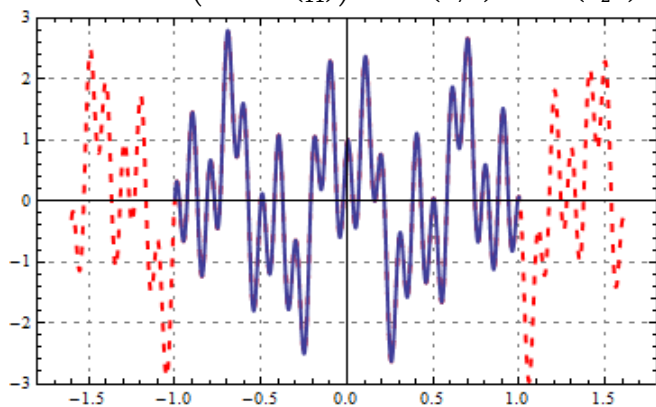
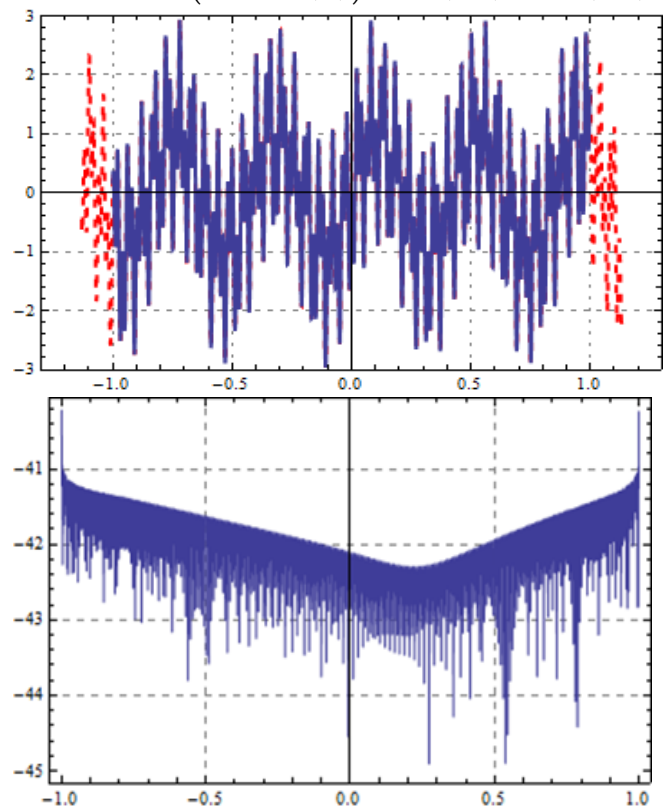


Figure 7.  $f_3(t)$  original [solid] and extrapolated [dashed] (top), logarithm of absolute error (bottom two) versus time; LPFs set 1 used.

$$4) f_4(t) = \cos\left(100\pi t - \left(\frac{\pi}{11}\right)\right) + \sin\left(\frac{33\pi t}{7}\right) - \cos\left(\frac{75\pi t}{2}\right)$$



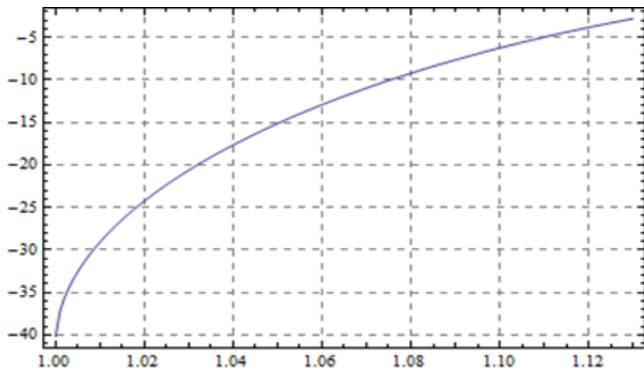


Figure 8.  $f_4(t)$  original [solid] and extrapolated [dashed] (top), logarithm of absolute error (bottom two) versus time; LPFs set 2 used.

5)  $f_5(t) = e^{-\pi(t-1)^2} + e^{-\pi(t+1)^2}$

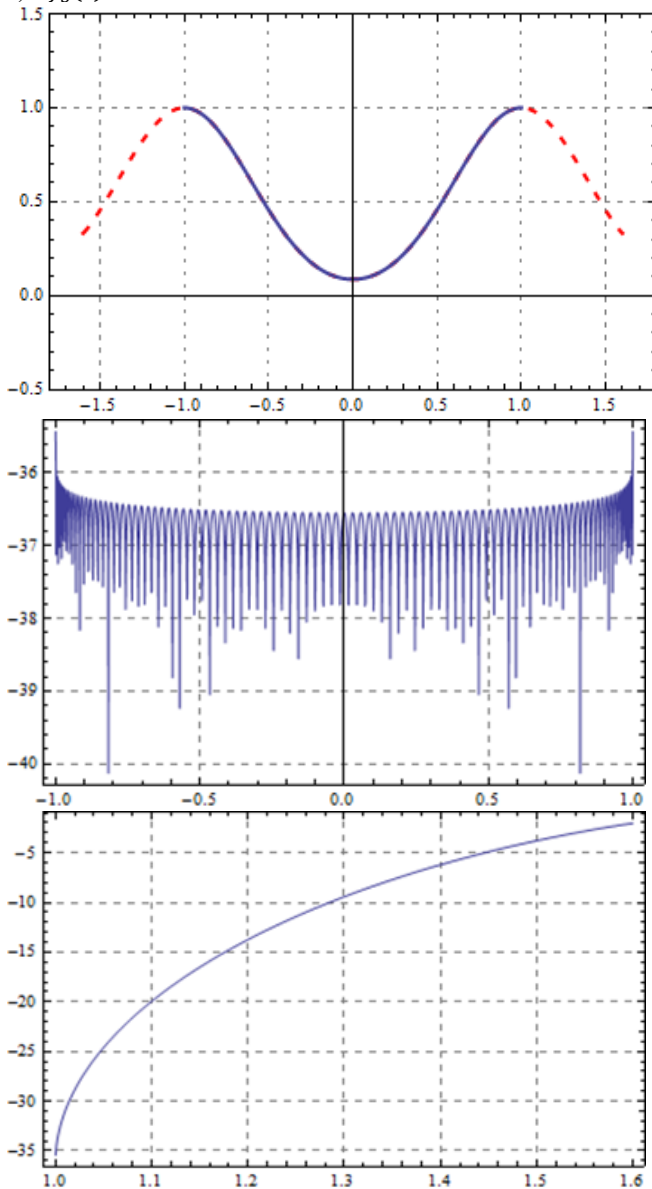


Figure 9.  $f_5(t)$  original [solid] and extrapolated [dashed] (top), logarithm of absolute error (bottom two) versus time; LPFs set 1 used.

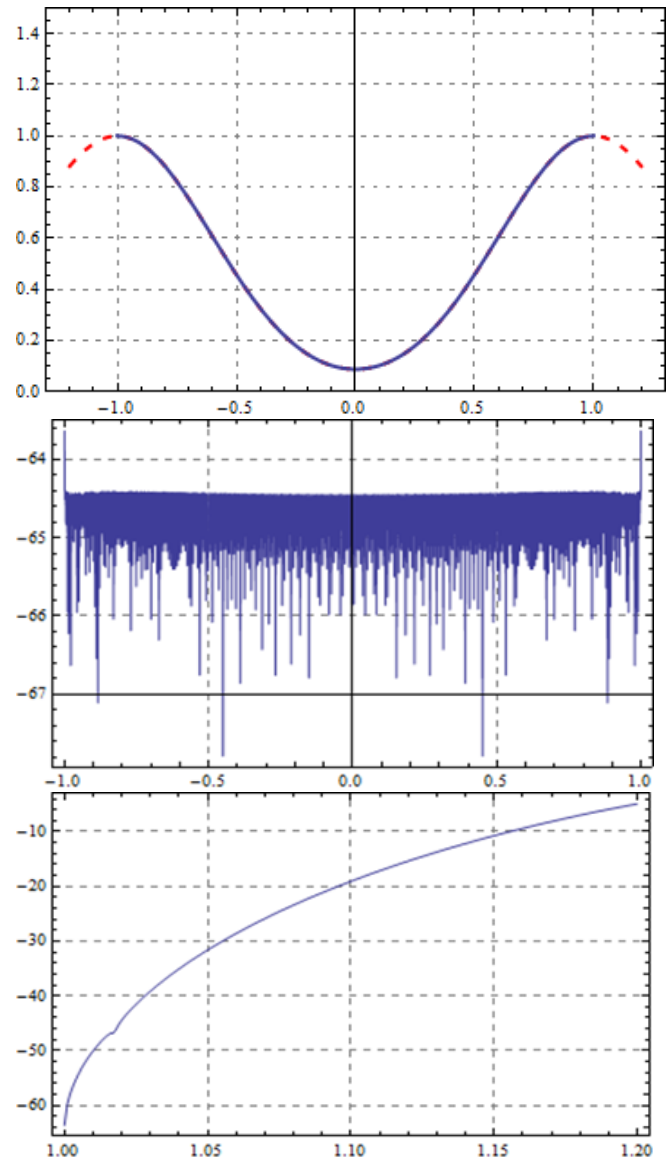
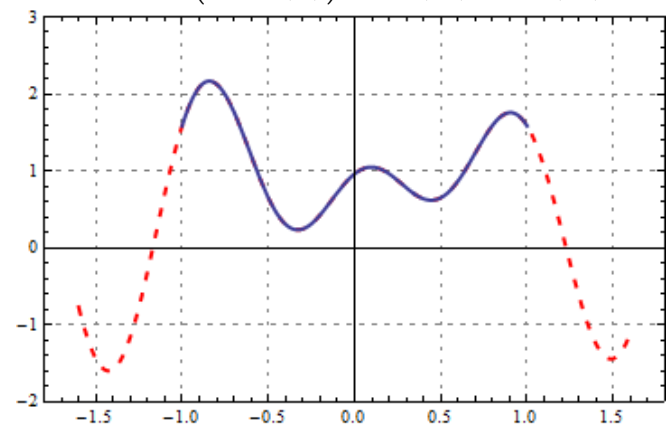


Figure 10.  $f_5(t)$  original [solid] and extrapolated [dashed] (top), logarithm of absolute error (bottom two) versus time; LPFs set 2 used.

6)  $f_6(t) = \cos\left(2\pi t - \left(\frac{\pi}{11}\right)\right) + \cos\left(\frac{2\pi t}{7}\right) - \cos\left(\frac{3\pi t}{2}\right)$



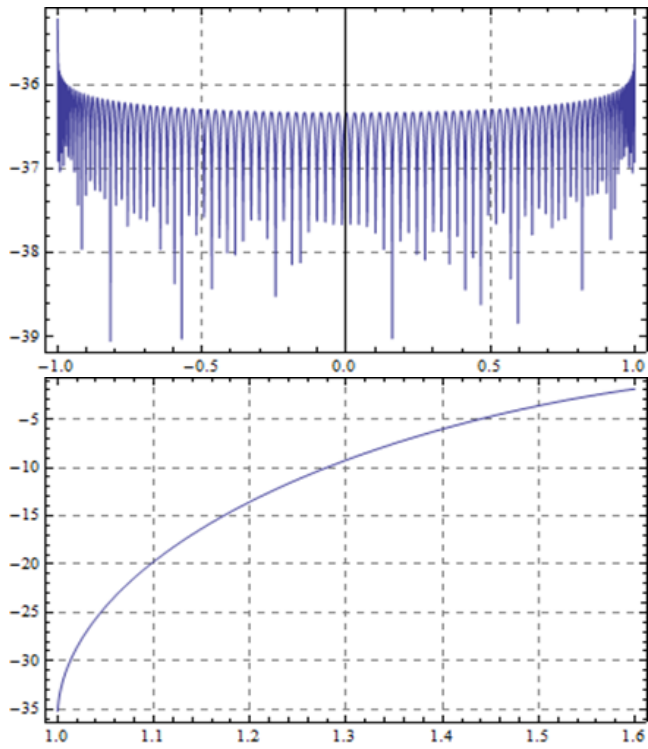


Figure 11.  $f_6(t)$  original [solid] and extrapolated [dashed] (top), logarithm of absolute error (bottom two) versus time; LPFs set 1 used.

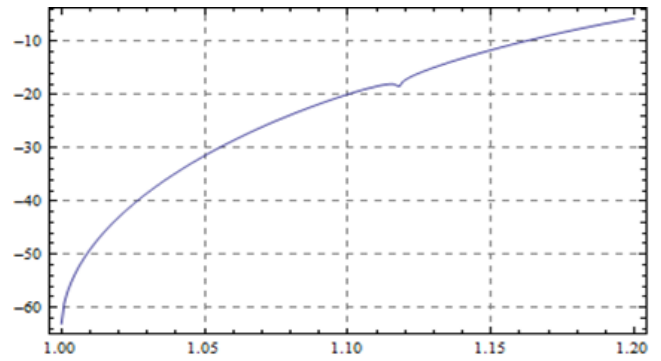
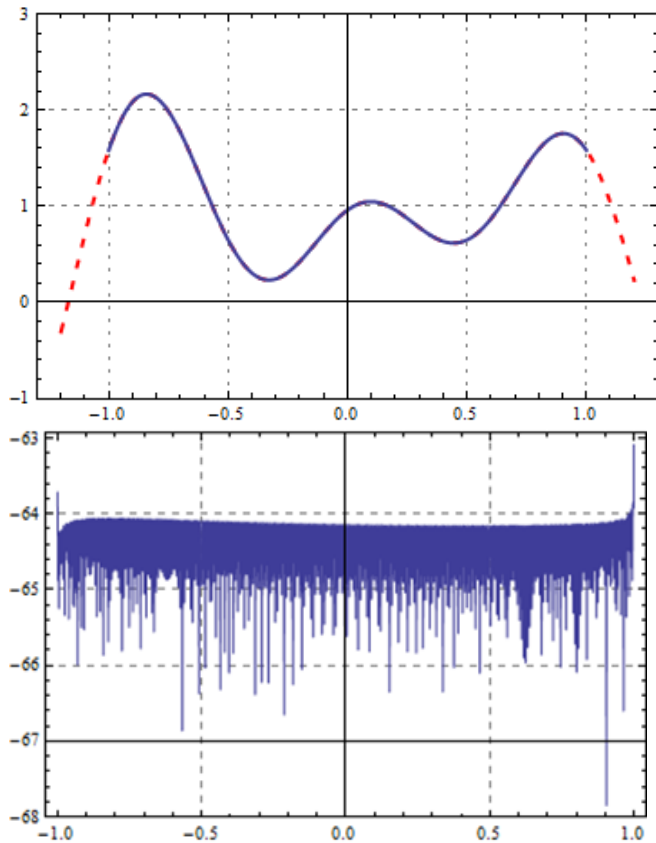


Figure 12.  $f_6(t)$  original [solid] and extrapolated [dashed] (top), logarithm of absolute error (bottom two) versus time; LPFs set 2 used.

$$7) f_7(t) = \frac{20}{\pi} e^{j2t^2} \text{sinc}\left(\frac{20t}{\pi}\right)$$

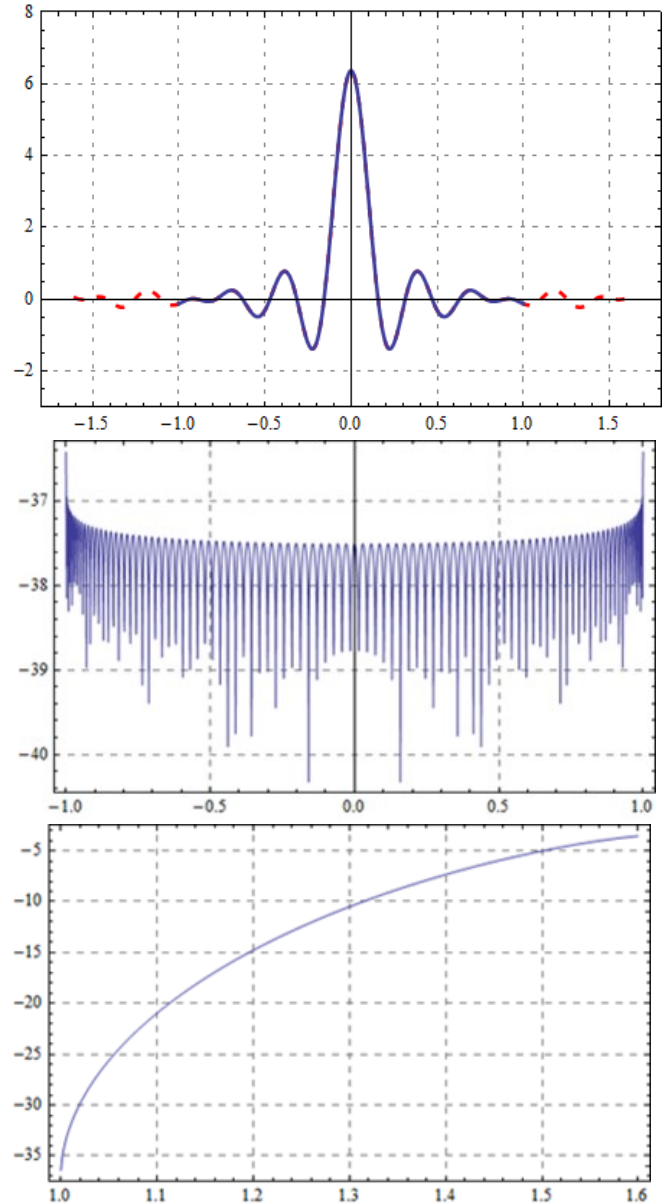


Figure 13. Real part of  $f_7(t)$  original [solid] and extrapolated [dashed] (top), logarithm of absolute error (bottom two) versus time; LPFs set 1 used.

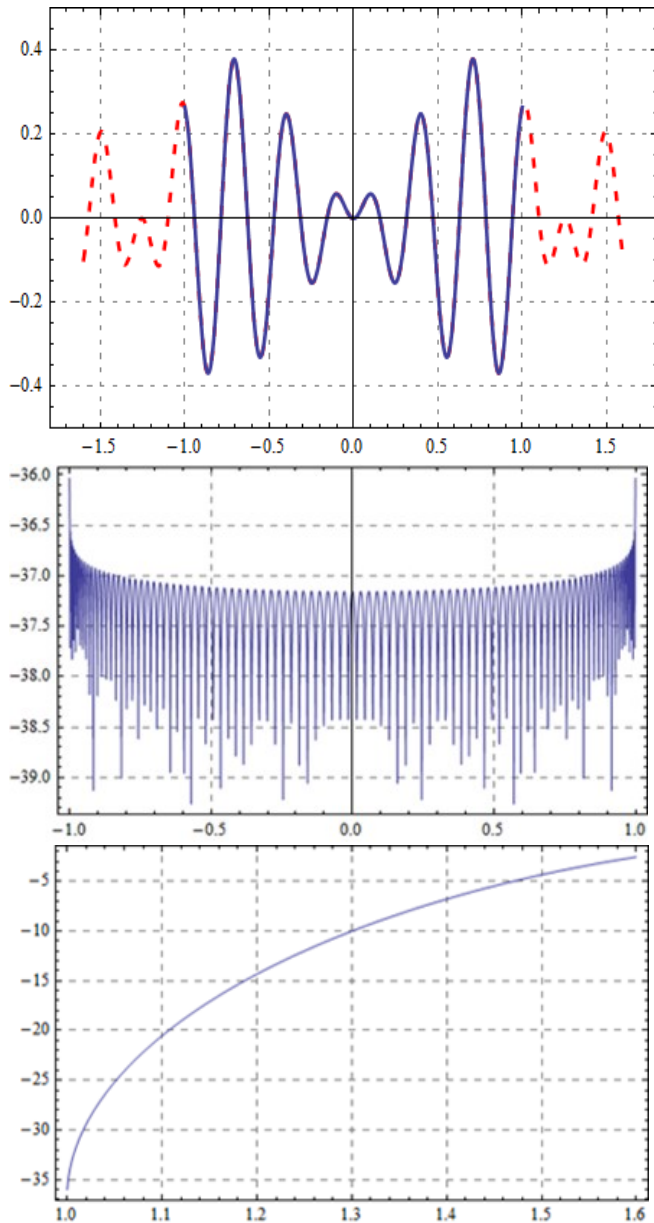


Figure 14. Imaginary part of  $f_7(t)$  original [solid] and extrapolated [dashed] (top), logarithm of absolute error (bottom two) versus time; LPFs set 1 used.

As mentioned earlier, we also performed extrapolation on an LCT bandlimited signal to compare our method with existing ones. We chose the same signal used by Shi *et al.* in [17]. It is given by the function  $f_7(t)$  (the *sinc* function used is a normalized *sinc* function) in the results. The extrapolation and error analysis for the real and imaginary parts of the signal are shown in Figures 13 and 14, respectively. The performance was measured using an error norm known as the normalized mean-square error (NMSE); following their [17] notation it is defined as:

$$NMSE = \frac{\|f_e - f\|^2}{\|f\|^2}, \quad (16)$$

where  $f_e$  is the extrapolated signal and  $f$  is the original signal. The NMSE of the extrapolated signal using our algorithm is  $8.430 \times 10^{-7}$ . The corresponding NMSE using the iterative algorithm proposed in [17] is  $1.037 \times 10^{-4}$ , and NMSE using the generalized PSWFs expansion method

proposed in [18] is only 0.685. Thus our algorithm is shown performs superiorly even for LCT bandlimited signals despite the fact that it is not the primary objective of this paper.

## V. CONCLUSION

We have presented an implemented robust and efficient algorithm for bandlimited signal extrapolation valid up to basically an arbitrarily high range of frequencies. Even though the algorithm is complex in the sense that it involves time consuming calculations and tedious computations with big matrices of very high precision, the overall idea is simple and easy to execute, thanks to the current computational speeds and available system memory. We believe that the accuracy with which the LPFs were computed with very high precision allowed this method to work efficiently thus making it suitable for extrapolating signals within the prescribed bandwidth. Characterizing the Slepian functions (LPFs set) finely and precisely into an appropriate polynomial expression is the key with which, this method could be extended to other LPF sets. During the characterization process, emphasis should be on incorporating more higher order ( $n$ ) terms in the synthesis equation (13) thus making  $N$  sufficiently large for extrapolation. This is a promising development in the field of signal processing [15-17,29,30] and will be helpful in the characterization of both known and random bandlimited observations. It should be stressed, however, that the key to the successful better-than-others results of our extrapolation algorithm is, indeed, the accurate numerical evaluations of linear prolate functions and their eigenvalues employing our proprietary robust algorithm for computing them.

## REFERENCES

- [1] M. Abramowitz, I. Stegun, Handbook of Mathematical Functions with Formulas, Graphs and Mathematical Tables, Addison-Wesley, New York, 1972.
- [2] D. Slepian, H.O. Pollack, "Prolate spheroidal wave functions, Fourier analysis, and uncertainty-I", Bell System Technical Journal, Vol 40, 43-63, 1961.
- [3] D. Slepian, Prolate spheroidal wave functions, Fourier analysis and uncertainty—IV: extensions to many dimensions; generalized prolate spheroidal functions, Bell Syst. Techn. J. 43 (1962) 3009–3057.
- [4] D. Slepian, Some asymptotic expansions for prolate spheroidal wave functions, J. Math. Phys. 44 (1965) 99–140.
- [5] D. Slepian, Some comments on Fourier analysis, uncertainty and modeling, SIAM Rev. 25 (1983) 379\_393.
- [6] K. Khare, N. George, "Sampling theory approach to prolate spheroidal wave functions", J. Phys. A: Math. Gen. 36 (2003) 10011\_10021.
- [7] P. Kirby, "Calculation of spheroidal wave functions", Comput. Phys. Comm. 175 (7) (2006) 465\_472.
- [8] I.C. Moore, M. Cada, "Prolate spheroidal wave functions, an introduction to the Slepian series and its properties", Appl. Comput. Harmon. Anal. 16 (2004) 208-230.
- [9] H. Xiao, V. Rokhlin, N. Yarvin, "Prolate spheroidal wave functions, quadrature and interpolation", Inverse Problems 17 (2001) 805\_838.
- [10] S. Senay, L.F. Chaparro, A. Akan, Sampling and reconstruction of non-bandlimited signals using Slepian functions, in: EUSIPCO 2008, Lusanne, Switzerland, August 25–29, 2008.
- [11] S. Senay, L.F. Chaparro, L. Durak, Reconstruction of non-uniformly sampled time-limited signals using prolate spheroidal wave functions, Signal Processing 89 (December) (2009) 2585–2595.

- [12] S. Senay, J. Oh, L.F. Chaparro, Regularized signal reconstruction for level-crossing sampling using Slepian functions, *Signal Processing* 92 (2012) 1157–1165.
- [13] M. Moshinsky and C. Quesne, “Linear canonical transformations and their unitary representations,” *J. Math. Phys.*, vol. 12, pp. 1772–1783, Aug. 1971.
- [14] H. M. Ozaktas, Z. Zalevsky, and M. A. Kutay, *The Fractional Fourier Transform With Applications in Optics and Signal Processing*. New York: Wiley, 2000.
- [15] H. Zhao, R.Y.Wang, D.P.Song, D.P.Wu, An extrapolation algorithm for M-bandlimited signals, *IEEE Signal Processing Letters* 18 (12) (2011) 745–748.
- [16] H. Zhao, et al., Extrapolation of discrete bandlimited signals in linear canonical transform domain, *Signal Processing* (2013), <http://dx.doi.org/10.1016/j.sigpro.2013.06.001>.
- [17] J. Shi, X. Sha, Q. Zhang, N. Zhang, Extrapolation of bandlimited signals in linear canonical transform domain, *IEEE Transactions on Signal Processing*, Vol. 60, No. 3, March 2012.
- [18] H. Zhao, Q. W. Ran, J. Ma, and L. Y. Tan, “Generalized prolate spheroidal wave functions associated with linear canonical transform”, *IEEE Trans. Signal Process.*, vol. 58, no. 6, pp. 3032–3041, June 2010.
- [19] R. Gerchberg, “Super-resolution through error energy reduction,” *Opt. Acta.*, vol. 12, no. 9, pp. 709–720, Sept. 1974.
- [20] A. Papoulis, “A new algorithm in spectral analysis and band-limited extrapolation,” *IEEE Trans. Circuit Syst.*, vol. CAS-22, no. 9, pp. 735–742, Sep. 1975.
- [21] L. Gosse, “Effective band-limited extrapolation relying on Slepian series and  $\ell^1$  regularization”, *Computers and Mathematics with Applications* 60 (2010) 1259-1279.
- [22] E.J. Candès, Compressive sampling, in: *Proceedings of the International Congress of Mathematicians, Madrid, Spain, 2006*.
- [23] E.J. Candès, The restricted isometry property and its implications for compressed sensing, *C. R. Acad. Sci. Paris, Ser. I* 346 (2008) 589-592.
- [24] M. Cada, Private communication, Department of Electrical and Computer Engineering, Dalhousie University, Halifax, NS, B3H 4R2, Canada, 2012.
- [25] C. Flammer, *Spheroidal Wave Functions*, Stanford Univ. Press, Stanford, CA, 1956.
- [26] V. Rokhlin, H. Xiao, Approximate formulae for certain prolate spheroidal wave functions valid for large values of both order and band-limit, *Appl. Comput. Harmon. Anal.* 22 (2007) 105–123.
- [27] Kaw Autar, Kalu Egwu E., and Nguyen Duc, *Numerical Methods With Applications: Abridged*, Lulu, 2nd ed., 2011.
- [28] A. Devasia, M. Cada, “Extrapolation of bandlimited signals using Slepian functions”, *Lecture Notes in Engineering and Computer Science: Proceedings of The World Congress on Engineering and Computer Science 2013, WCECS 2013, 23-25 October, 2013, San Francisco, USA*, pp492-497.
- [29] Kauppinen, K. Roth, “Audio signal extrapolation-theory and applications”, in *proc. (DAFx-02), Hamburg, Germany, September 26-28, 2002*.
- [30] A. Kaup, K. Meisinger, T. Aach, “Frequency selective signal extrapolation with applications to error concealment in image communication”, *Int. J. Electron. Commun.*, Vol 59, 147-156, 2005.